Molecular Biology of the Cell
Vol. 16, 4992–5003, October 2005

Dual Interaction of JAM-C with JAM-B and $\alpha_M\beta_2$ Integrin: Function in Junctional Complexes and Leukocyte Adhesion[D]

Chrystelle Lamagna,* Paolo Meda,† Guillaume Mandicourt,* James Brown,‡ Robert J.C. Gilbert,§ E. Yvonne Jones,‡ Friedemann Kiefer,‖ Pilar Ruga,† Beat A. Imhof,* and Michel Aurrand-Lions*

Departments of *Pathology and Immunology and †Cell Physiology and Metabolism, Centre Médical Universitaire, 1204 Geneva, Switzerland; ‡Division of Structural Biology and §Cancer Research UK Receptor Structure Group, Henry Wellcome Building of Genomic Medicine, Headington, Oxford OX3 7BN, United Kingdom; and ‖Max-Planck-Institute for Molecular Biomedicine, Institute for Vascular Cell Biology, D-48149 Münster, Germany

Submitted April 13, 2005; Revised July 5, 2005; Accepted August 2, 2005
Monitoring Editor: Ben Margolis

The junctional adhesion molecules (JAMs) have been recently described as interendothelial junctional molecules and as integrin ligands. Here we show that JAM-B and JAM-C undergo heterophilic interaction in cell-cell contacts and that JAM-C is recruited and stabilized in junctional complexes by JAM-B. In addition, soluble JAM-B dissociates soluble JAM-C homodimers to form JAM-B/JAM-C heterodimers. This suggests that the affinity of JAM-C monomers to form dimers is higher for JAM-B than for JAM-C. Using antibodies against JAM-C, the formation of JAM-B/JAM-C heterodimers can be abolished. This liberates JAM-C from its vascular binding partner JAM-B and makes it available on the apical side of vessels for interaction with its leukocyte counterreceptor $\alpha_M\beta_2$ integrin. We demonstrate that the modulation of JAM-C localization in junctional complexes is a new regulatory mechanism for $\alpha_M\beta_2$-dependent adhesion of leukocytes.

INTRODUCTION

Junctional adhesion molecules (JAMs) are immunoglobulin (Ig)-like proteins, consisting of two extracellular Ig domains, a short cytoplasmic tail and a PDZ-domain-binding motif (Ebnet *et al.*, 2004). JAM-A is a component of tight junctions in both epithelial and endothelial cells and regulates monocyte transmigration (Malergue *et al.*, 1998; Martin-Padura *et al.*, 1998). We and others have described two closely related molecules, JAM-B and JAM-C, both expressed by endothelial cells and localized at intercellular contacts (Aurrand-Lions *et al.*, 2000; Cunningham *et al.*, 2000; Aurrand-Lions *et al.*, 2001a). *Trans*-homophilic interaction of JAM-A between adjacent cells is required for its proper localization at cell-cell contacts (Bazzoni *et al.*, 2000a). The structural study of crystallized JAM-A has confirmed that the protein forms homodimers, which organize in a zipperlike structures at intercellular contacts (Kostrewa *et al.*, 2001; Prota *et al.*, 2003). Similarly, it has been suggested that JAM-C molecules need *trans*-homophilic interaction to be correctly localized at cell-cell borders (Aurrand-Lions *et al.*, 2001b).

In mouse, JAM-B and JAM-C expression is restricted to noncirculating cells, including vascular and lymphatic endothelial cells (Aurrand-Lions *et al.*, 2001b). In human, JAM-C is also expressed by platelets and activated T lymphocytes and it has been suggested that JAM-C mediates the adhesion of lymphocytes to endothelial cells via JAM-B expressed on the vascular bed (Cunningham *et al.*, 2000; Arrate *et al.*, 2001). However, JAM-B/JAM-C interaction may also occur between adjacent endothelial cells.

Members of the JAM family have been shown to interact with leukocyte integrins. Ostermann and collaborators have reported that the membrane proximal domain of JAM-A on endothelial cells binds to the I domain of the leukocyte integrin LFA-1 ($\alpha_L\beta_2$) (Ostermann *et al.*, 2002; Fraemohs *et al.*, 2004). This interaction supports the adhesion and transmigration of T lymphocytes (Ostermann *et al.*, 2002). Although JAM-A mainly localizes at cell-cell contacts in endothelial cells, it is redistributed to the apical surface upon inflammatory conditions, suggesting that JAM-A may become available for LFA-1-mediated leukocyte interaction (Ozaki *et al.*, 1999; Ebnet *et al.*, 2004). Similarly, human JAM-C expressed on platelets participates in the binding of platelets to leukocytes, by interacting with the I domain of the leukocyte integrin $\alpha_M\beta_2$ (Mac-1) (Santoso *et al.*, 2002; Chavakis *et al.*, 2004). Finally, human JAM-B interacts with

This article was published online ahead of print in *MBC in Press* (http://www.molbiolcell.org/cgi/doi/10.1091/mbc.E05–04–0310) on August 10, 2005.

[D] The online version of this article contains supplemental material at *MBC Online* (http://www.molbiolcell.org).

Address correspondence to: Michel Aurrand-Lions (Michel.Aurrand-Lions@medecine.unige.ch).

Abbreviations used: JAM, junctional adhesion molecule; FRAP, fluorescence recovery after photobleaching; EGFP, enhanced green fluorescent protein; HEV, high endothelial venules; FACS, fluorescence-activated cell sorting; ROI, region of interest; DLS, dynamic light scattering; AUC, analytical ultracentrifugation.

the integrin $\alpha_4\beta_1$ expressed by T lymphocytes (Cunningham *et al.*, 2002). This interaction only occurs after prior engagement of JAM-B with JAM-C and is not detectable in cells in which JAM-C expression is absent (Cunningham *et al.*, 2002). In all the cases, these findings indicate that the JAM family members participate to the recruitment of leukocytes at inflammatory sites.

However, the interactions between JAM and integrin do not explain how the leukocyte will cope with the JAMs expressed on endothelial cells in vivo. More precisely, what happens when the monocyte integrin $\alpha_M\beta_2$ faces JAM-B and JAM-C, both expressed by vascular and lymphatic endothelial cells (Aurrand-Lions *et al.*, 2001b)? One can imagine that a more complex network of interactions mediated by JAMs occurs between leukocytes and endothelial cells. Several questions regarding the significance of JAM-B and JAM-C interactions between endothelial cells, as well as their effect on leukocyte recruitment, remain to be answered.

In the present study, we investigate whether JAM-C is differentially recruited at intercellular contacts by homophilic or heterophilic interactions with JAM-B. Using fluorescence recovery after photobleaching (FRAP) experiments we demonstrate that JAM-B recruits and stabilizes JAM-C at cell-cell contacts. We are able to disrupt this interaction and modify JAM-C localization by means of antibody directed against JAM-C. In addition, we show that JAM-C localization modulates $\alpha_M\beta_2$ integrin-dependent adhesion to the endothelium.

MATERIALS AND METHODS

Expression Vectors Encoding Chimeric Molecules Fused to EGFP or FLAG-tag Sequences

FLAG-JAM-B, JAM-C-EGFP, and soluble JAM-C comprising the two extracellular domains have been previously described (Aurrand-Lions *et al.*, 2001a, 2001b). The soluble JAM-B and the soluble JAM-C V domain (solJAM-C 1d) were obtained by PCR using the same cloning strategy. Primers were obtained from Microsynth (Microsynth GmbH, Balgach, Switzerland), and restriction sites added for cloning strategy are underlined. The cDNA encoding the extracellular V domain of JAM-C was amplified using plasmid encoding the full-length sequence of murine JAM-C, Pfu polymerase, T7, and (5′-gctctagacagtgttgccgtcttgcctacag-3′) as forward and reverse primers. The PCR product was digested with *Hin*dIII and *Xba*I before cloning in pcDNA3 containing FLAG-tag sequence (Wiedle *et al.*, 1999). Similarly, the cDNA encoding soluble JAM-B was obtained by PCR using (5′-tcagctaggcagccagct-3′) and (5′-gctctagaatctacttgcattcgcttcc-3′) as forward and reverse primers. The PCR product digested with *Xba*I was then cloned in frame with the FLAG-tag sequence in pcDNA3 using *Eco*RI/blunt and *Xba*I sites. For the generation of JAM-C-EGFP-Out (^{EGFP}JAM-C), a three-step cloning strategy was used. Starting from the vector encoding soluble JAM-C, the sequence was excised by *Hin*dIII/*Xba*I and cloned in pcDNA-3 devoid of FLAG-tag sequence. The sequence encoding the EGFP was then amplified using (5′-gctctagagtgagcaagggcgaggagctg-3′) as forward primer modified with *Xba*I site and (5′-ctaagggcccttctcgagctcgtccatgccgagag-3′) as reverse primer modified by *Xho*I and *Apa*I sites. PCR product was digested with *Xba*I and *Apa*I, and subcloned in frame with the sequence encoding the V and C_2 domains of JAM-C using *Xba*I and *Apa*I sites. This resulted in a second intermediate product encoding soluble JAM-C fused to EGFP. The remaining sequence encoding the transmembrane and cytoplasmic part of JAM-C was amplified using (5′-gagccgctcgagttgaacattgctgggattattgg-3′) and (5′-ctagggcccctcagataacaaaggacgatttgtg-3′) as forward and reverse primers. PCR product was subcloned in the vector comprising the soluble JAM-C fused to EGFP after *Xho*I/*Apa*I digestion. The EGFP was inserted to the hinge region between the membrane proximal C_2 domain and the transmembrane part of JAM-C (^{EGFP}JAM-C). This construct left intact the two extracellular domains, the phosphorylation sites and the PDZ-binding-domain motif in the cytoplasmic tail. The sequence encoding PECAM-1-EGFP has been previously described (Wong *et al.*, 2000). Integrity of expression constructs was verified by sequencing the cDNA on both strands using Dual Lycor 4000 (MWG, Ebersberg, Germany).

Antibodies

The panel of rat monoclonal antibodies (CRAM panel) against mouse JAM-C (H33, H36, F26, and D22) and rat monoclonal antibodies against mouse PECAM-1/CD31 (GC51) and mouse Mac-1/CD11b (M1/70) were previously described (Springer *et al.*, 1979; Piali *et al.*, 1993; Aurrand-Lions *et al.*, 2001a). Anti-human CD44 (Hermes, 9B5) used as irrelevant antibody control rat IgG_{2a} was kindly provided by Dr. B. Engelhardt (Berg *et al.*, 1991; Laschinger and Engelhardt, 2000). Polyclonal rabbit sera against murine JAM-B or JAM-C were generated using recombinant soluble molecules consisting in the two extracellular Ig domains and have been previously described (Gliki *et al.*, 2004; Lamagna *et al.*, 2005).

Production of FLAG-tagged Soluble Molecules

293T cells were transiently transfected with pcDNA3 plasmids containing coding sequences for soluble domains of JAM-B or JAM-C by calcium-phosphate precipitation. Producing cells were kept under confluent conditions in DMEM with 2% Ultroser (BioSepra S.A., Ciphergen BioSystems, Cergy-saint-Christophe, France), and the supernatant was collected after 10 d (Legler *et al.*, 2001). FLAG-tagged molecules were purified from supernatant using a M2 affinity column (Sigma-Aldrich, Saint-Louis, MO) and then competitively eluted with FLAG-peptide (Sigma-Aldrich) according to the manufacturer's instructions. Eluted proteins were dialyzed against phosphate-buffered saline (PBS).

Cell Lines, Transfections, and Mixed Coculture Experiments

The WEHI78/24 monocytoid cell line and the bEnd.5 endothelioma cell line were kindly provided by B. Engelhardt (Bern University, Switzerland). LyEnd.1, bEnd.5, and WEHI78/24 were cultured in DMEM and Chinese hamster ovary (CHO) cells in F12 medium (GIBCO, Invitrogen, Basel, Switzerland), both supplemented with antibiotics and 10% fetal calf serum (FCS). Fugen 6 (Roche, Rotkreuz, Switzerland) was used according to the manufacturer's recommendation for stable transfection. Cells were cultured in the presence of 1 mg/ml Geneticin (GIBCO, Invitrogen) to select for stable expressing cells. Expressing cells were selected using fluorescence-activated cell sorting (FacStar, Becton Dickinson, Mountain View, CA) after immunostaining with appropriate antibodies. Mixed cocultures were obtained by mixing cells as indicated and growing them to confluence over a 2- to 3-d period.

Immunofluorescence Staining

For immunohistochemistry with monoclonal antibody (mAb) anti-JAM-C (F26), polyclonal antibodies against JAM-B or JAM-C, frozen sections were fixed with acetone/methanol 1:1 for 5 min at −20°C, dried, and rehydrated in PBS, 0.2% Gelatin, and 0.05% Tween 20. Sections were incubated with primary antibody for 1 h at room temperature and, after three washes in PBS, incubated with a secondary antibody coupled to FITC or Texas Red dye (Jackson ImmunoResearch Laboratories, West Grove, PA). Nuclei were visualized using TO-PRO-3 according to manufacturer's instruction (Molecular Probes, Eugene, OR). Note that antibodies-treated lymph nodes were harvested from mice 24 h after a single injection of 150 μg of antibodies and frozen in OCT. Immunostaining was done using the anti-JAM-C polyclonal antibody.

For immunocytochemistry, cells were fixed with cold methanol for 5 min before washing with PBS, 0.2% bovine serum albumin (BSA). Cells were then incubated with primary polyclonal rabbit serum or M2 anti-FLAG mAb (Sigma-Aldrich) for 1 h and washed, before further incubation with secondary antibodies coupled to Texas Red (Jackson ImmunoResearch Laboratories). Images were acquired using confocal microscope Zeiss LSM510 (Zeiss, Oberkochen, Germany).

ELISA Assays on Mixed Cocultures

For ELISA assay on mixed CHO monolayers, cells grown to confluency in 96-well plates were fixed with 4% paraformaldehyde without further permeabilization. JAM-C was then detected using the polyclonal antibody, anti-rabbit antibody coupled to peroxidase and ABTS (Sigma Chemical). The relative signal intensity calculated on sextupliquette was normalized to the signals obtained with monolayers of ^{EGFP}JAM-C-expressing cells. The signals obtained in the absence of ^{EGFP}JAM-C-expressing cells (0/100%) correspond to the background values obtained with monolayers of JAM-B-expressing cells or nontransfected cells. In Figure 2D, the values obtained for the mix of ^{EGFP}JAM-C with JAM-B-transfected cells were expressed relative to the signals obtained at the same cell ratio with the mix of ^{EGFP}JAM-C with nontransfected CHO cells (Figure 2C).

FRAP Analysis

Zeiss LSM 510 confocal microscope equipped with a temperature controller and CO_2 ventilation module was used. Bleaching of the outlined regions of interest (ROIs) was done at 37°C with the 488-nm argon laser line at 50% power, full transmission, for 5–8 iterations (35–56 s). Observation of the recovery was done at 50% laser power and 3.1% transmission to avoid significant photobleaching over the period of observation. Openlab software was used to measure pixel intensity in the ROIs. The fluorescence intensity just after the bleach (I_{bleach}) was between 5 and 20% of the prebleach fluo-

rescence (100%). The normalized results expressed in percent were obtained by calculation of the fractional recovery: $R_{Frac}(t) = (R(t) - I_{bleach})/(1 - I_{bleach})$ (Axelrod *et al.*, 1976). The half time to raise 50% of the full recovery value ($t_{1/2}$) and mobile fraction were estimated from nonlinear regression fitting to experimental curves (Yguerabide *et al.*, 1982). Normalized results were obtained from at least four independent experiments and three to four ROIs analyzed for each acquisition.

Flow Cytometry

FLAG-tagged murine soluble JAM-C or JAM-B were incubated with JAM-C-EGFP- or JAM-B-EGFP-transfected MDCK mixed with nontransfected MDCK as internal control (1:1) on ice. After washing with PBS, 0.2% BSA binding of soluble JAM was detected using biotynilated M2 anti-FLAG mAb (Sigma-Aldrich) and streptavidin-phycoerythrin (BD-PharMingen, San Diego, CA).

LyEnd.1 and bEnd.5 were incubated with polyclonal sera against JAM-C or JAM-B on ice. After washing with PBS, 0.2%, BSA binding of antibodies was detected using a phycoerythrin-coupled anti-rabbit antibody (Jackson ImmunoResearch Laboratories). As control, preimmune sera were used. Analysis was performed using FACSCalibur and Cellquest Software (Becton Dickinson).

Pulldown Experiments and Western Blots

Confluent monolayers of MDCK cells transfected with either murine JAM-C-EGFP or murine JAM-B-EGFP were washed with PBS before lysis with 50 mM Tris, 150 mM NaCl, 1% Triton (TNT) containing protease inhibitors (Complete, Roche). Recombinant soluble molecules were loaded onto beads coupled to the M2 anti-FLAG antibody (Sigma-Aldrich). After washing, beads coupled to soluble molecules were incubated with cell lysates overnight at 4°C. For blocking experiments, 50 μg/ml antibodies were added during incubation. Beads were washed three times with TNT, boiled with reducing buffer, and subjected to SDS-PAGE. Proteins were transferred onto a nitrocellulose filter (Amersham Pharmacia Biotech GmbH, Freiburg, Germany) by electroblotting. The filter was blocked overnight at 4°C with 5% milk in PBS, 0.05% Tween 20 and incubated in the same buffer with monoclonal anti-EGFP antibody (Covance, Berkeley Antibody Company, Richmond, CA). Blots were revealed with a horseradish peroxydase-conjugated anti-mouse antibody (Jackson ImmunoResearch Laboratories) and ECL peroxydase substrate.

LyEnd.1 and bEnd.5 cells were grown to confluence in 6-cm Petri dishes, washed three times in PBS and surface biotinylated with PBS containing 0.1 mM $CaCl_2$, 1 mM $MgCl_2$, and 0.4 mg/ml sulfo-NHS-biotin for 30 min at room temperature. Biotinylation reaction was blocked in DMEM, 5% FCS for 5 min at room temperature. After three washes with PBS, cells were lysated with 50 mM Tris, pH 8.0, 150 mM NaCl, 0.5% Np-40 containing protease inhibitors on ice for 10 min. Lysates were immunoprecipitated with either preimmune rabbit sera, anti-JAM-C rabbit serum, or anti-JAM-B rabbit serum preincubated with protein G Sepharose 4 fastflow. Sepharose beads were washed three times with lysis buffer and boiled in reducing buffer. Samples were run on a 10% SDS-PAGE gel and transferred onto nitrocellulose membrane. Biotinylated proteins were revealed with chemiluminescence using HRP-labeled streptavidin.

Dynamic Light Scattering and Analytical Ultracentrifugation

The molecular weights of murine soluble JAM-B and JAM-C were investigated by dynamic light scattering (DLS) and analytical ultracentrifugation (AUC). In DLS, scattering intensity is proportional to the hydrodynamic radius, allowing estimation of the molecular weights and conformations of macromolecules in solution. Samples of JAM-B, JAM-C, and an equimolar JAM-B/JAM-C mixture were prepared in tris-buffered saline (TBS; 20 mM Tris, pH 7.4, 150 mM NaCl) at concentrations of 1 mg/ml, centrifuged to remove particulate material, and added to a quartz sample cell placed in a DynaPro99 dynamic light scattering instrument (Protein Solutions, Lakewood, NJ). Scattering measurements taken at 20°C were analyzed using the DYNAMICS software package (Protein Solutions), and molecular weights were estimated by comparing measurements of the hydrodynamic radius those of known globular proteins.

To further investigate the molecular weights and oligomeric nature of soluble murine JAM proteins, sedimentation equilibrium experiments were performed in a Beckman Optima XL-I analytical ultracentrifuge (Fullerton, CA), essentially as previously described (Ikemizu *et al.*, 2000). Briefly, JAM-B, JAM-C, or an equimolar mixture of JAM-B and JAM-C in TBS were used at concentrations ranging from 0.2 to 0.8 mg/ml, centrifuged at 10,000, 12,000, or 18,000 rpm at 20°C and imaged using absorbance optics at 254-, 280-, and 290-nm wavelengths and using interference optics. The sample distributions measured at equilibrium were fitted with the program ULTRASPIN using a single-species equation (Altamirano *et al.*, 2001). Any nonideal behavior, such as self-association, manifests itself as increasing apparent whole-cell weight-average molecular weights (M_w) with increasing concentration.

Real-time Quantitative PCR

Peripheral lymph nodes were harvested from nontreated C57Bl/6 J0 mice (Charles River, St. Alban les Elbeuf, France) or mice injected with monoclonal antibodies (150 μg/mice) after 24 h. RNA was extracted by Trizol according to the manufacturer's instructions (GIBCO, Invitrogen). Reverse transcription was done by using 1 μg of total RNA, random hexanucleotide primers and Superscript II reverse transcriptase (Invitrogen). One in 25 dilution of the resulting cDNA was used for real-time quantitative PCR using the SYBR Green PCR Master Mix kit as recommended by the provider and an ABI PRISM 7900HT Sequence Detection System (Applied Biosystems, Foster City, CA). The following primers were used: JAM-C forward ($^{5'}$-gctgggagagcacatgcaa-$^{3'}$), reverse ($^{5'}$-caggagctctgggctcaca-$^{3'}$); RPS-9 forward ($^{5'}$-gaccaggagctaaagttgattgga-$^{3'}$), reverse ($^{5'}$-tcttggccagggtaaacttga-$^{3'}$); TBP forward ($^{5'}$-ttgacctaaagaccattgcacttc-$^{3'}$), reverse ($^{5'}$-ttctcatgatgactgcagcaaa-$^{3'}$). JAM-C relative expression level was normalized by geometric averaging of internal control genes RPS-9 and TBP according to Vandesompele *et al.* (2002).

Stamper-Woodruff Assays on Peripheral Lymph Node Sections

Peripheral lymph nodes were harvested from nontreated C57Bl/6 J0 mice (Charles River) or from mice injected with monoclonal antibodies (150 μg/mice) and frozen in OCT. Fresh 10-μm sections were cut and used within 30 min. The Stamper-Woodruff assays were performed as described in Stamper and Woodruff (1976). Briefly, WEHI78/24 cells were harvested in plateau phase (2.0–2.5 $\times$ 10^6 cells per ml), stained with Calcein-AM according to the manufacturer's instructions (Molecular Probes), and suspended in DMEM in presence or absence of 10 μg/ml monoclonal antibodies against JAM-C (H36, D22, and H33, all IgG2a isotypes), α_M (CD11b; M1/70, IgG2b isotype), α_4 (CD49d; PS/2, IgG2b isotype) or an isotype-matched control antibody to JAM-C antibodies (anti-human CD44; 9B5, IgG2a). WEHI78/24 cells, (5 $\times$ 10^5), were added to cryosections within a 8-μm diameter ring and allowed to adhere for 30 min under constant agitation at 37°C. Nonadherent cells were removed by three washes in Hanks' balanced salt solution (HBSS) supplemented with 2 mM Ca^{2+} and 2 mM Mg^{2+}, and slides were placed in HBSS glutaraldehyde 2%, 2 mM Ca^{2+}, and 2 mM Mg^{2+} for 15 min. Sections were examined under fluorescent microscopy, and the number of adherent cells per mm^2 of lymph node was determined.

Immunogold Electron Microscopy

Peripheral lymph nodes from two control and two H33 antibody-treated mice were fixed for 5 min at room temperature in 4% paraformaldehyde and 0.1% glutaraldehyde, followed by a 60-min fixation in 4% paraformaldehyde (all fixatives diluted in 0.1 M phosphate buffer, pH 7.4). After three washes in 0.1 M phosphate buffer, tissues were embedded in 12% gelatin and cooled on ice. Small blocs of gelatin-embedded tissues were infused with 2.3 M sucrose, frozen in liquid nitrogen, and sectioned with a EMFCS cryoultramicrotome (Leica, Cambridge Ltd, England). Ultrathin sections were mounted on Parlodion-coated copper grids. The sections were processed according to a previously described protocol (Liou *et al.*, 1996; Tokuyasu, 1997), which, in these experiments, included a 1-h exposure at room temperature to the anti-JAM-C polyclonal antibody (diluted 1:1000), and a 20-min exposure at room temperature to goat anti-rabbit antibody conjugated to 10-nm gold particles, diluted 1:10. Cryosections were screened and photographed in a CM10 electron microscope (Philips, Eindhoven, The Netherlands). As negative controls, sections were exposed to either the preimmune serum or to only the gold-conjugated goat antibody. None of these incubations resulted in a sizable, specific staining of the sections.

To assess the distribution of JAM-C immunolabeling, we photographed 40 randomly selected endothelial cell profiles featuring a nucleus. All photographs were taken at the original magnification of $\times$21,000. Prints made at the final magnification of $\times$63,000 were used to measure the length of plasma membrane (control antibody, 453 μm; H33 antibody, 510 μm) and the area of cytoplasm (control antibody, 297 μm^2; H33 antibody, 494 μm^2), using an ACECAD Professional graphic tablet connected to a Quantimet Leica 500+ system (Leica). After scoring the number of gold particles over the measured compartments, we calculated the number of particles per μm of membrane and μm^2 of cytoplasm. We further evaluated the distribution of gold particles over the junctional portions of the cell membrane, which were identified by a narrowing of the intercellular space between two adjacent cell membranes associated to an accumulation of microfilaments on the cytoplasmic sides.

Values were expressed as mean $\pm$ SEM (numerical density of particles over cell membrane and cytoplasm, which showed a Gaussian distribution) or as median values (number of particles per junctional region, which showed a highly asymmetrical distribution), and compared by analysis of variance (numerical density of particles) or nonparametric statistics (labeling of junctional regions), as provided by the Statistical Package for Social Sciences (SPSS, Chicago, IL).

Statistical Analysis

Each bar in graphs represents the mean $\pm$ the SE of measurement (SEM). All experiments, excepted the morphometric analysis of immunoelectron microscopy as described above, were evaluated with the Mann-Whitney's t test, using the statistical software StatView (Abacus Concepts, Berkeley, CA). A value of $p < 0.05$ was considered as statistically significant.

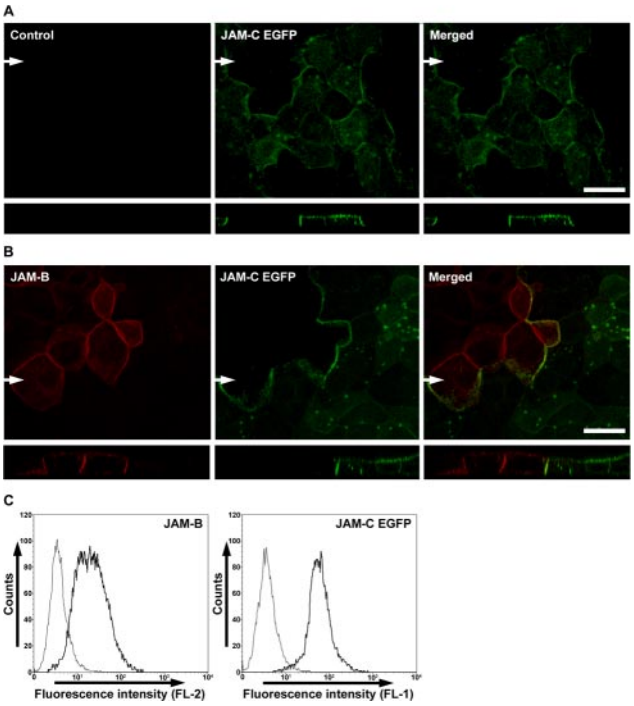

Figure 1. JAM-C is recruited at cell-cell contacts by JAM-B. FLAG-JAM-B- and JAM-C-EGFP-transfected MDCK cells were mixed and the localization of the molecules was visualized by immunofluorescent labeling. (A) Negative control for JAM-B staining with polyclonal rabbit antibody and anti-rabbit Texas red probe. (B) Plane view of stacked series of pictures (top panel), JAM-C-EGFP is enriched in JAM-C/JAM-B intercellular contacts. On the *Z*-axis analysis (bottom panel), JAM-C appears to be localized in basolateral contacts when engaged heterophilically with JAM-B contacts. Arrows indicate the *Z*-axis. Scale bar, 20 μm. (C) Surface expression of JAM-B and JAM-C EGFP on MDCK cells used in A and B. The thin line represents the negative control obtained by omitting the primary antibody; bold line represents surface expression of JAM-B or JAM-C EGFP, as indicated.

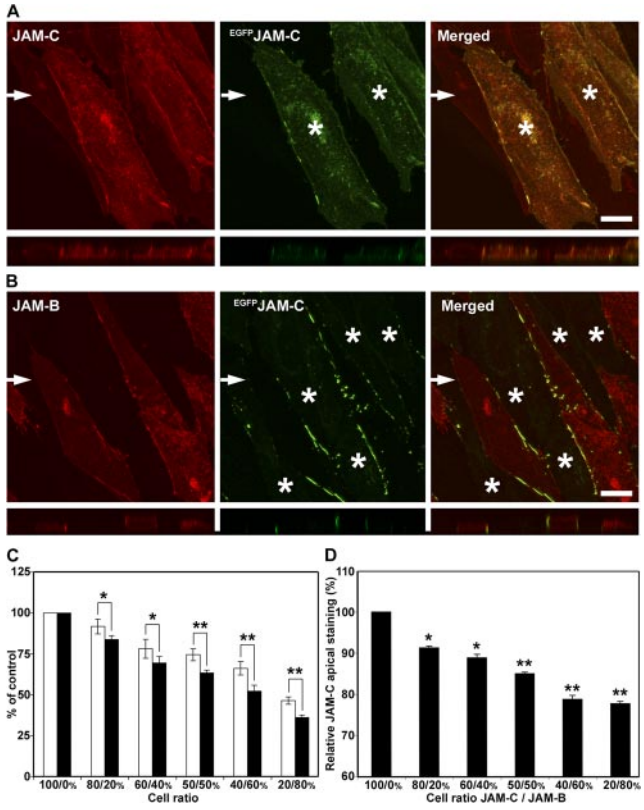

Figure 2. Recruitment of JAM-C at cell-cell contacts depletes the apical pool of the protein. (A) CHO cells transfected with ^{EGFP}-JAM-C (green) were mixed with JAM-C full-length (red) or (B) JAM-B-expressing cells (red) and stained with polyclonal antibodies against murine JAM-B or JAM-C. The plane view of stacked series of images and *Z*-axis reconstitution show that ^{EGFP}JAM-C is enriched in JAM-C/JAM-B intercellular contacts as compared with JAM-C/JAM-C intercellular contacts. Arrows indicate the *Z*-axis. Scale bar, 20 μm. (C) Quantification by ELISA of ^{EGFP}JAM-C expressed on the apical cell surface. ^{EGFP}JAM-C-transfected CHO cells were mixed with JAM-C (white columns) or JAM-B-expressing cells (black columns) at indicated cell ratios. The protein ^{EGFP}JAM-C at the apical cell surface was detected with an anti-JAM-C polyclonal antibody. (D) Same as B, but signals were normalized to the ones obtained with mixed monolayers of JAM-C-expressing cells with nontransfected cells. As shown, the relative JAM-C signal detected at the apical cell surface is decreased when the percentage of JAM-B-positive cells is increased. Each bar represents the mean value ± SEM (n = 6) of one representative experiment observed in at least three separate experiments. (* $p < 0.05$, ** $p < 0.01$).

RESULTS

JAM-C Is Recruited to Cell-Cell Junctions by JAM-B

We investigated whether JAM-B/JAM-C or JAM-C/JAM-C interactions differentially contribute to the localization of JAM-C in cell-cell contacts. To this end we cocultured JAM-C-EGFP- and JAM-B-transfected MDCK epithelial cells and studied the subcellular localization of JAM-C (Figure 1, A and B). Using confocal microscopy, we found that JAM-C was enriched at contacts between JAM-C-EGFP- and JAM-B-expressing cells, whereas JAM-B was distributed over the surface of the cell. The analysis of *z*-axis views revealed that the apical pool of JAM-C was apparently reduced in cells adjacent to JAM-B-expressing cells. This was probably due to the recruitment of JAM-C to the junctional region because MDCK-transfected cells expressed homogenous levels of JAM-C-EGFP (Figure 1C).

To ensure that these observations were not a consequence of polarized junctional complexes in MDCK cells, similar coculture experiments were performed with cells devoid of tight junctions. CHO cells expressing full-length JAM-B or JAM-C were mixed with cells expressing JAM-C fused to the green fluorescent protein (^{EGFP}JAM-C). The ^{EGFP}JAM-C was poorly enriched at contacts with neighboring JAM-C-expressing cells (Figure 2A). In contrast, ^{EGFP}JAM-C was enriched in cell-cell contacts with JAM-B-expressing cells (Figure 2B). To proof that JAM-C was recruited away from the apical surface by JAM-B, we quantified JAM-C at the apical surface of mixed monolayers by ELISA (Figure 2C). Although paraformaldehyde fixation might cause some cell permeabilization, the signals gradually decreased when JAM-C-expressing cells were mixed with JAM-B cells at increasing ratios. The inhibition of the apical JAM-C signal was maximal when 60% of JAM-B-expressing cells were admixed (Figure 2D). To exclude that JAM-C was internalized instead of being concentrated at junctions, surface expression of ^{EGFP}JAM-C was analyzed by flow cytometry after coculture with JAM-B- or JAM-C-expressing cells (Supplementary Figure 1). No significant loss of surface staining was observed when ^{EGFP}JAM-C-transfected cells were cultured with JAM-B compared with JAM-C-expressing cells,

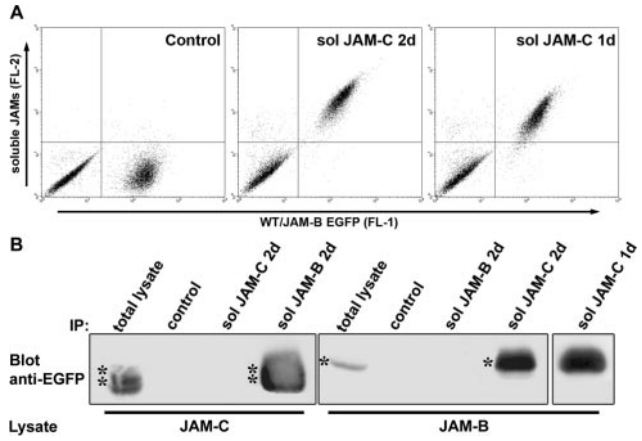

Figure 3. JAM-C interacts heterophilically with JAM-B through its V domain, and monomeric JAM-B dissociates JAM-C homodimers to form heterodimers. (A) JAM-B-EGFP-transfected MDCK cells were mixed with nontransfected cells and stained with soluble JAM-C consisting in the two extracellular domains (2d) or the membrane distal V domain (1d) alone. Dot plots represent the EGFP fluorescence intensity (FL1) and the fluorescence intensity due to binding of soluble molecules (FL2). The soluble JAM-C 2d as well as the soluble JAM-C 1d binds to JAM-B-EGFP-transfected cells. No binding was observed on nontransfected cells as depicted by the absence of FL2 signal on EGFP-negative cells. Negative control obtained by omitting primary antibody against the flag-tag is shown. (B) Cell lysates obtained from JAM-C-EGFP- or JAM-B-EGFP-transfected MDCK cells were precipitated with beads coupled to soluble JAM-B or soluble JAM-C. Western blots were revealed using anti-EGFP antibody. Soluble JAM-C 2d, as well as soluble JAM-C 1d, and soluble JAM-B are able to pull-down JAM-B-EGFP and JAM-C-EGFP, respectively. Control of loading was obtained using M2 anti-FLAG antibody (unpublished data).

showing that JAM-B did not induce JAM-C internalization. This suggested that JAM-B was able to recruit and interact with JAM-C at cell-cell contacts.

JAM-C Interacts Heterophilically with JAM-B through Its V Domain

To demonstrate a direct molecular interaction between JAM-C and JAM-B, we produced recombinant soluble molecules comprising the extracellular V and C_2 (2d) or V (1d) Ig domains of JAM-C. These molecules were assessed for their capacity to bind cells transfected with JAM-B using flow cytometry (Figure 3A). Nontransfected cells were used as internal control to set the compensation settings. No bleeding of EGFP fluorescence was observed in the FL-2 channel used to detect the bound soluble molecules. In contrast, the strong signals observed in the FL-2 channel for EGFP expressing cells incubated with solJAM-C 2d or sol-JAM-C 1d showed that both soluble molecules interacted efficiently with JAM-B-transfected cells. To provide a conclusive proof of JAM-B/JAM-C interaction, we determined whether soluble JAM-C or JAM-B was able to precipitate cellular JAM-B or JAM-C from lysates (Figure 3B). Our results indicated that soluble JAM-C pulled down cellular JAM-B and vice versa. It was remarkable that neither JAM-C/JAM-C nor JAM-B/JAM-B homophilic interactions were detectable by this technique. Interestingly, the V domain of JAM-C was sufficient to bind and precipitate JAM-B.

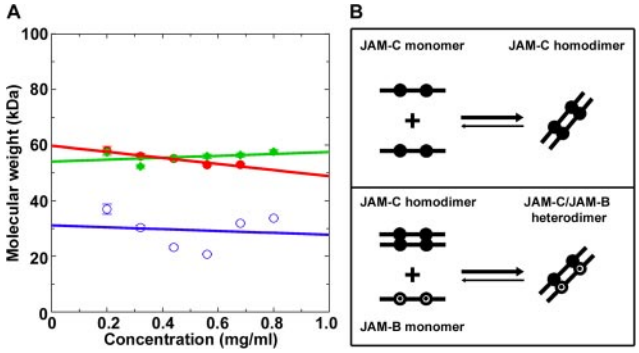

Figure 4. Monomeric JAM-B dissociates JAM-C homodimers to form JAM-B/JAM-C heterodimers. (A) Representative plots of apparent whole-cell weight-average molecular weight (M_w) against sample concentration (mg/ml) for absorbance data at 280 nm and 12 000 rpm. Open blue circles are for JAM-B, red circles are for JAM-C, and green diamonds are for an equimolar JAM-B/JAM-C mixture. Fitted curves are for a linear regression of weight with concentration as appropriate for a dimerization process (Ikemizu *et al.*, 2000). (B) Schematic representation of JAM-B/JAM-C heterodimerization. In solution, JAM-C tends to form homodimers (top panel). In the presence of JAM-B molecule, JAM-B/JAM-C heterodimers are preferentially formed. This interpretation does not account for parallel or antiparallel heterodimerization.

JAM-B Dissociates JAM-C Homodimers to Form JAM-B/JAM-C Heterodimers

Soluble JAM-B, JAM-C, and mixed JAM-B/JAM-C molecules were analyzed by dynamic light scattering (DLS). The estimated molecular weights were 47.6, 67, and 72.6 kDa, respectively. The standard curve used in this estimation assumed spherical proteins and might slightly overestimate molecular weights of nonspherical tandem arrangements of Ig-like domains expected for JAM-B and JAM-C. Comparison of SDS-PAGE and DLS-derived molecular weight estimations suggested that JAM-C and the JAM-B/JAM-C mixture formed dimers. In contrast, JAM-B had a significantly lower DLS-based molecular weight, indicative of monomers (unpublished data).

To further investigate the dimerization properties of JAM-C, we performed analytical ultracentrifugation (AUC) at different speeds using a range of concentrations of JAM-B, JAM-C, or an equimolar mixture of JAM-B/JAM-C (Figure 4A and Supplementary Figure 2). With JAM-C, a straight line revealing an inverse trend of apparent M_w in the range of 55–60 kDa was observed at different concentrations. This was a typical nonideal behavior arising from crowding effects at higher sample concentrations and allowed extrapolation to infinite dilution, giving a M_w of 59,812 ± 787 Da in the absence of these effects (Ikemizu *et al.*, 2000). This clearly showed that JAM-C was a tightly associated dimer. However, JAM-B displayed a range of values of M_w at varying concentrations, all clustered in the region of 30 kDa. Given the behavior of JAM-B in SDS-PAGE, the results suggested that JAM-B was predominantly monomeric and unlike the data for JAM-C, there was no indication of dimerization. In contrast, when an equimolar mixture of JAM-B and JAM-C was subjected to the same analysis, there was a direct relationship between the total protein concentration and the M_w. This showed that JAM-B, while monomeric itself, substituted JAM-C/JAM-C homodimers to form JAM-B/JAM-C heterodimers (Figure 4B). Thus both dynamic light scattering and analytical ultracentrifugation experiments indicated a clear preference for JAM-B/JAM-C heterodimer formation.

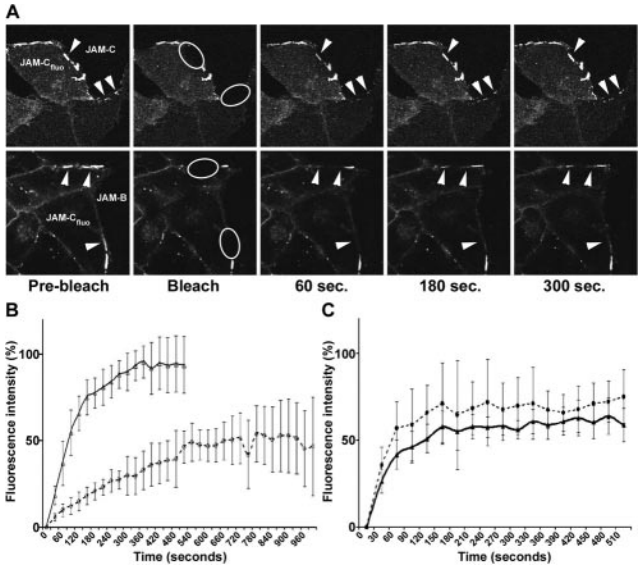

Figure 5. Dynamic of JAM-C junctional recruitment by JAM-B in CHO-transfected cells. (A) ^{EGFP}JAM-C CHO cells were mixed with JAM-B CHO cells at a ratio 1:1. FRAP experiments of ^{EGFP}JAM-C engaged in homophilic interaction (top panel) or heterophilic interaction (bottom panel) were performed. Regions of interest for bleaching were drawn on contacts between ^{EGFP}JAM-C-expressing cells and nonfluorescent cells (ellipses). Arrowheads underline clusters of ^{EGFP}JAM-C in which the recovery occurred. Elapsed time after photobleaching is indicated. Scale bars, 10 μm. (B) Fractional recovery curves obtained for ^{EGFP}JAM-C/JAM-C (plain curve, open triangles) or ^{EGFP}JAM-C/JAM-B (dashed curve, open circles) junctional complexes. Recovered fluorescence is expressed as function of time elapsed after photobleaching (time 0). (C) Fractional recovery curves obtained for PECAM-EGFP/JAM-C (plain curve, filled triangles) or PECAM-EGFP/JAM-B (dashed curve, filled circles) cell-cell contacts are shown. No significant differences can be observed between the two recovery curves indicating that the differences observed in B are due to *trans*-interaction between ^{EGFP}JAM-C and its binding partners JAM-B or JAM-C. The curves are mean values ± SD obtained from at least four independent experiments and three to four regions of interest analyzed for each acquisition.

It has been reported that dimerization of JAM-A is partially mediated by a glutamic acid residue in the V domain (E60; Kostrewa *et al.*, 2001). We therefore mutated the analogous putative dimerization motif in the V domain of soluble 1d and 2d forms of JAM-C (E66R) and tested their capacity to bind JAM-B (Supplementary Figure 3). Binding of the mutated V/C_2 form to JAM-B was reduced compared with nonmutated JAM-C molecule. In addition, the mutated V domain was unable to bind JAM-B. These experiments indicated that the V domain of JAM-C was sufficient to interact with JAM-B and that the C_2 domain probably stabilized this interaction.

The Dynamics of JAM-C at Intercellular Junctions Is JAM-B Dependent

We investigated the dynamics of JAM-C engaged in JAM-C/JAM-C homophilic or JAM-C/JAM-B heterophilic interactions at cell-cell contacts. For this purpose we performed fluorescence recovery after photobleaching (FRAP) experiments using mixed monolayers of ^{EGFP}JAM-C- and JAM-B-transfected cells (Figure 5A). Photobleaching was performed on intercellular junctions. In homophilic JAM-C/JAM-C contacts, fluorescence was recovered within 300 s, whereas heterophilic JAM-C/JAM-B contacts recovered much slower and never reached the maximum level of fluorescence (Figure 5A). Recovery curves obtained after fractional fitting showed that the mobile fraction (M_f) of ^{EGFP}JAM-C was reduced in heterophilic compared with homophilic clusters (M_f: 52% vs. 94%, Figure 5B). The half recovery time of ^{EGFP}JAM-C in junctional clusters ($t_{1/2}$) was more than 2.5 times longer when ^{EGFP}JAM-C/JAM-B cell-cell contacts were compared with ^{EGFP}JAM-C/JAM-C junctions. Such a difference could be explained by two mechanisms: 1) JAM-C was immobilized by JAM-B in cell-cell contacts; 2) JAM-B-expressing cells exhibited a decreased membrane fluidity that limited the diffusion rate of JAM-C on neighboring cells. To exclude the latter mechanism, we performed FRAP experiments using mixes of either JAM-B- or JAM-C-expressing cells with CHO cells transfected with a different junctional protein (PECAM-1-EGFP). As shown in Figure 5C, we observed that the recovery of PECAM-1-EGFP in cell-cell contacts with JAM-B- or JAM-C-expressing cells was similar. These results clearly indicated that JAM-B immobilized JAM-C in junctional complexes and inhibited the exchange of JAM-C with the nonjunctional pool of the protein.

Vascular and Lymphatic Endothelial Cells Show Different Expression Levels of JAM-B and JAM-C

The expression of JAM-B and JAM-C was analyzed on sections of peripheral lymph nodes. Although JAM-C was predominantly expressed by lymphatic sinuses, JAM-B was more prominent on high endothelial venules (HEVs). However, both molecules were expressed by lymphatic and vascular structures and were partially colocalized (Figure 6A). To confirm this differential expression we compared the endothelioma cell line bEnd.5 with the lymphangioma cell line LyEnd.1 (Supplementary Figure 4). In agreement with histological observations, JAM-B was expressed at higher levels by blood vascular cells bEnd.5 compared with lymphatic cells LyEnd.1 (Figure 6B). In contrast, JAM-C was expressed by both cell lines. These results were confirmed by Western blotting as shown in Figure 6C. These observations suggested that JAM-C and JAM-B were differentially expressed in lymphatic and vascular endothelial cells.

Anti-JAM-C Antibody Blocks JAM-B/JAM-C Interaction and Modulates JAM-C Localization on Endothelial Cells In Vivo

We tested monoclonal antibodies against JAM-C for their ability to interfere with JAM-B/JAM-C interaction. Pull-down experiments with soluble JAM-C were performed in the presence of antibodies. One of the antibodies (H33) blocked JAM-B/JAM-C interaction, whereas others had only partial or no effect (Figure 7A). We thus investigated whether anti-JAM-C blocking antibody affected the localization of the molecule in vivo. Mice were injected with anti-JAM-C antibodies and the distribution of the protein in lymph nodes was analyzed by immunohistochemistry (Figure 7B). The blocking antibody H33 induced the appearance of a diffuse JAM-C staining, whereas the partial blocking antibody D22 showed an intermediate effect and the non-blocking antibody H36 did not change the pattern of JAM-C distribution. To exclude that these observations were due to an increase in JAM-C expression, real-time quantitative PCR experiments were performed with lymph node RNA extracts from mice treated with antibodies against JAM-C (Figure 7C). Antibodies did not significantly modify relative JAM-C expression levels, enforcing the hypothesis that H33 antibody treatment resulted in the redistribution of JAM-C on endothelial cells in vivo.

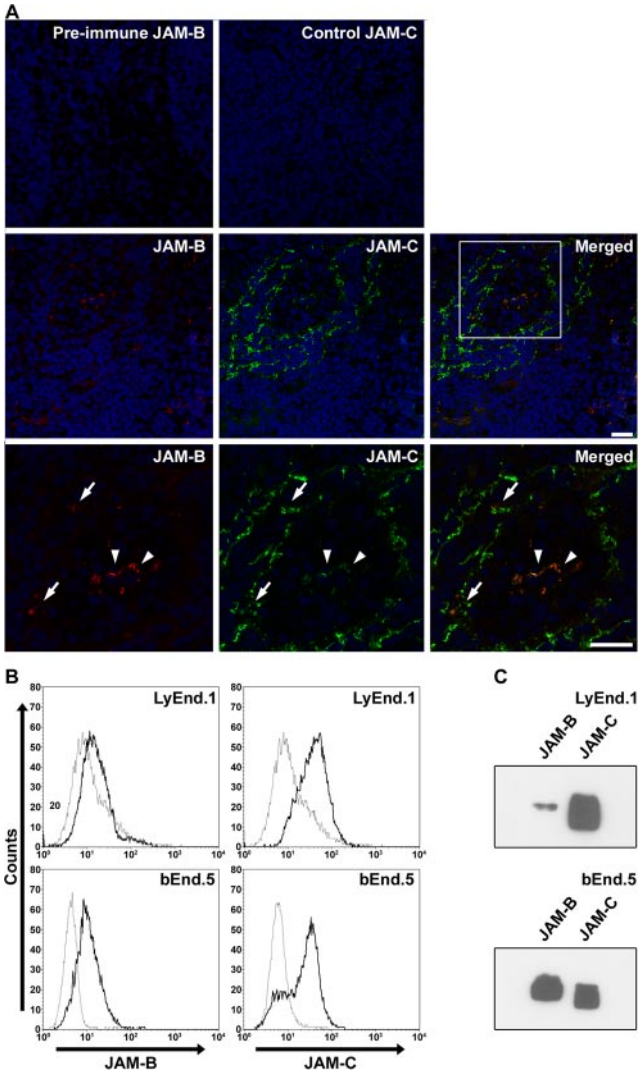

Figure 6. JAM-C is predominantly expressed by lymphatic vessels, whereas JAM-B is prominent in vascular endothelial cells. (A) Double staining for JAM-B (red) and JAM-C (green) performed on murine peripheral lymph node sections shows that JAM-C is highly expressed on lymphatic sinuses (arrows), whereas JAM-B is strongly expressed by HEVs. Higher magnification (bottom panel) shows that JAM-B and JAM-C are both expressed on high endothelial venules where they partially colocalize (arrowheads). Negative control obtained with preimmune rabbit serum against JAM-B or by omitting primary antibody against JAM-C are shown. Scale bar, 20 μm. (B) The expression levels of JAM-B and JAM-C molecules by the lymphangioma cell line LyEnd.1 (Supplementary Figure 4) and the endothelioma cell line bEnd.5 were analyzed by FACS. JAM-C expression is predominant in LyEnd.1, whereas JAM-B is preferentially expressed by endothelial cells from blood origin. (C) JAM-B and JAM-C expressions by LyEnd.1 (top panel) and bEnd.5 (bottom panel) were analyzed by Western blot and enforced the results observed by FACS.

To proof this hypothesis, immunoelectron labeling of JAM-C was performed on ultrathin sections from antibody-treated mice. Vascular regions were determined according to morphological criteria, and the expression of JAM-C by endothelial cells in lymph nodes was confirmed. In control and H33 antibody-treated groups, JAM-C immunolabeling predominated at the cell membrane of endothelial cells (Figure 8). Quantitative analysis showed that the membrane labeling was increased by 25% after treatment with the H33 antibody, under conditions that did not significantly modify the cytoplasmic labeling (Table 1). Evaluation of the distribution of the membrane labeling along the interacting lateral membranes of adjacent cells, revealed that most junctional regions were immunolabeled for JAM-C in the control samples (Table 1). In contrast, much less junctional regions were immunolabeled in H33-treated samples (17.7% vs. the control value of 67.1%), under conditions that did not impair the labeling of adjacent, nonjunctional domains of the same lateral membranes (Table 1 and Figure 8). Thus, these data showed that the anti-JAM-C antibody H33 redistributed JAM-C away from vascular junctions to the apical membrane.

Redistribution of JAM-C Induced by Anti-JAM-C Blocking Antibody Increases Monocyte Adhesion to Lymph Node Sections

We have shown that JAM-C localization in junctions is driven by its interaction with JAM-B. By blocking JAM-B/JAM-C hetero-dimerization with the antibody H33, we induced the redistribution of JAM-C in vivo. We thus addressed the question whether the antibody H33 would render JAM-C available for binding to its leukocyte counterreceptor $\alpha_M\beta_2$ integrin. For this purpose we performed adhesion assays using a monocytoid cell line (WEHI78/24) on lymph node sections (Stamper and Woodruff, 1976). These cells expressed α_M and α_4 integrins, respective ligands for JAM-C and JAM-B (Figure 9A). However, the monocytoid cell line did not express JAM-B or JAM-C. Adhesion assays were performed at 37°C in culture medium to allow integrin-dependent adhesion. Under these conditions the leukocytes predominantly adhered to lymphatic sinuses (Figure 9, B and C). Incubation of monocytoid cells with lymph node sections in the presence of anti-JAM-C antibodies did not significantly affect the adhesion (Figure 10A). We then performed the adhesion assay using lymph node sections from mice treated with anti-JAM-C antibodies (all rat IgG2a isotype). A significant increase of cell adhesion to lymph node sections was observed when mice were treated with the JAM-C/JAM-B blocking H33 antibody but not with the H36 or D22 antibodies (Figure 10B). Because all three antibodies were of the same isotype and directed against the same protein, this allowed excluding that this effect was due to Fcγ receptors. We then investigated whether $\alpha_4\beta_1$ or $\alpha_M\beta_2$ integrins (respective ligands for JAM-B and JAM-C) were responsible for the increased adhesion of monocytoid cells. Interestingly, the blocking antibody against $\alpha_M\beta_2$ was able to revert the H33-mediated increased adhesion of monocytoid cells to the basal level, whereas the anti-$\alpha_4\beta_1$ integrin antibody had no effect. Our results suggested that the engagement of JAM-C with $\alpha_M\beta_2$ was responsible for the increased adhesion. These experiments represented a paradigm for differential function of JAM-C. When JAM-C was not engaged with JAM-B in endothelial cell-cell contacts it became available for interactions with leukocyte $\alpha_M\beta_2$ integrin.

DISCUSSION

JAM-B Recruits and Stabilizes JAM-C at Interendothelial Junctions

The JAM family members were initially described as adhesion molecules localized at cell-cell contacts (Martin-Padura *et al.*, 1998; Bazzoni *et al.*, 2000a; Aurrand-Lions *et al.*, 2001b). The C-terminus of the JAMs contains a PDZ-domain-bind-

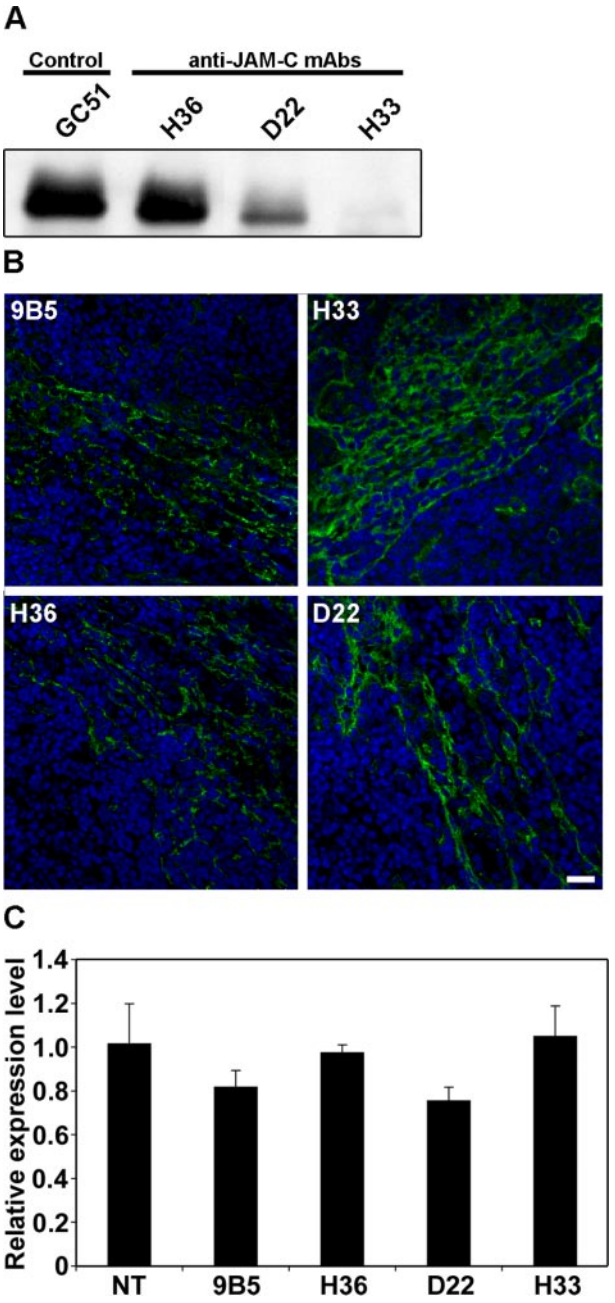

Figure 7. Anti-JAM-C mAb blocks JAM-B/JAM-C interaction and modulates JAM-C localization. (A) Cell lysates obtained from JAM-B-EGFP-transfected MDCK cells were precipitated with beads coupled to soluble JAM-C in the presence of irrelevant anti-PECAM antibody (GC51) or antibodies directed against JAM-C, as indicated. The presence of immunoprecipitated material was revealed by immunoblotting with antibody directed against EGFP. The anti-JAM-C antibody H33 abolishes JAM-C/JAM-B interaction. (B) Sections of lymph nodes harvested from mice treated with the indicated antibodies were stained with an anti-JAM-C polyclonal antibody (green) and for nuclei (blue). The H33 antibody, which affects JAM-B/JAM-C interaction, induces redistribution of JAM-C as compared with the nonblocking anti-JAM-C antibody H36 or the isotype-matched control (9B5). This was observed on sections obtained from three different mice. One representative picture is shown. Scale bar, 20 μm. (C) Relative expression levels of JAM-C mRNA in lymph nodes from antibody-treated mice were quantified by real-time PCR. Treatment of animals with anti-JAM-C antibodies, and specifically H33 antibody, does not affect JAM-C expression by endothelial cells. Each bar represents the mean ± SEM of three mice. One representative experiment out of three.

ing motif, which mediates their interaction with tight junction scaffolding proteins, including ZO-1 (Bazzoni *et al.*, 2000b; Ebnet *et al.*, 2000, 2003). More recently it has been demonstrated that JAM-C interacts with polarity complex molecules such as PAR-3, PAR-6, or PATJ and regulates the activity of the small GTPase Cdc-42 (Ebnet *et al.*, 2003; Gliki *et al.*, 2004). Taken together, these findings indicate that JAM-C plays a role in the formation and maintenance of intercellular contacts.

In the present study, we demonstrate that *trans*-heterophilic binding between JAM-B and JAM-C occurs at intercellular contacts resulting in enrichment of JAM-C at cell-cell contacts. In contrast, enrichment of JAM-B at the JAM-B/JAM-C junctions does not occur. We suggest that JAM-B delivers a signal through JAM-C, which results in the stabilization of JAM-C at intercellular contacts. This is consistent with our previous finding that dephosphorylation of JAM-C on Ser 281 results in its enrichment at cell-cell borders (Ebnet *et al.*, 2003). When JAM-C is stabilized by JAM-B at cell-cell junctions, the number of accessible JAM-C molecules on the apical surface is reduced. Such an apical localization of JAM-C is in apparent contradiction with our previous findings that JAM-C is restricted to tight junctions of MDCK cells (Aurrand-Lions *et al.*, 2001a). This discrepancy relies probably on the culture conditions. Indeed, in the current study, cocultures were performed over a 2-d period to get homogenous mixes of JAM-B- and JAM-C-expressing cells, whereas our previous results were based on cultures performed over a period of 11 d (Aurrand-Lions *et al.*, 2001b). These observations are consistent with findings showing that molecules involved in the establishment and maintenance of polarity are targeted to membrane subdomains, depending on environmental and temporal cues (Roh *et al.*, 2002).

The interaction between JAM-B and JAM-C involves at least two different regions of the JAM-C molecule: an essential dimerization motif in the V domain (RIE_{66}) and the C_2 domain, which probably stabilizes the interaction (Supplementary Figure 3). It has been reported that the dimerization motif R(V,I,L)E in the V domain of JAM-A, which is common to the JAM family members, is responsible for *cis*-homodimerization of the protein (Kostrewa *et al.*, 2001). In the present study, we show that the V domain of JAM-C is sufficient to interact with JAM-B and that mutation of the putative dimerization motif of JAM-C (E66R) abolishes the interaction. In contrast with previous suggestions by Liang and collaborators, we have found that soluble JAM-C is present as homodimers, whereas soluble JAM-B is monomeric (Liang *et al.*, 2002). In addition, monomeric JAM-B competitively substitutes JAM-C in homodimers to form JAM-B/JAM-C heterodimers. Hence, the affinity of JAM-C for its heterodimerization with JAM-B is higher than the one for JAM-C homodimerization.

JAM-B and JAM-C molecules are differentially coexpressed by vascular and lymphatic endothelial cells (Palmeri *et al.*, 2000; Aurrand-Lions *et al.*, 2001b). The expression level of JAM-B is up-regulated during chronic inflammatory diseases, whereas JAM-C expression is not affected by inflammatory cytokines (Liang *et al.*, 2002). However JAM-C is recruited at interendothelial contacts of HUVECs upon inflammatory stimuli (Lamagna *et al.*, 2005). On the basis of our findings on JAM-B/JAM-C interaction, we suggest that the level of JAM-B expression regulates the distribution of JAM-C in cell-cell contacts under inflammatory conditions. Nevertheless, alternative mechanisms may participate to the stabilization of JAM-C at cell-cell junctions in cells devoid of JAM-B expression. Indeed it has been shown that PAR-3,

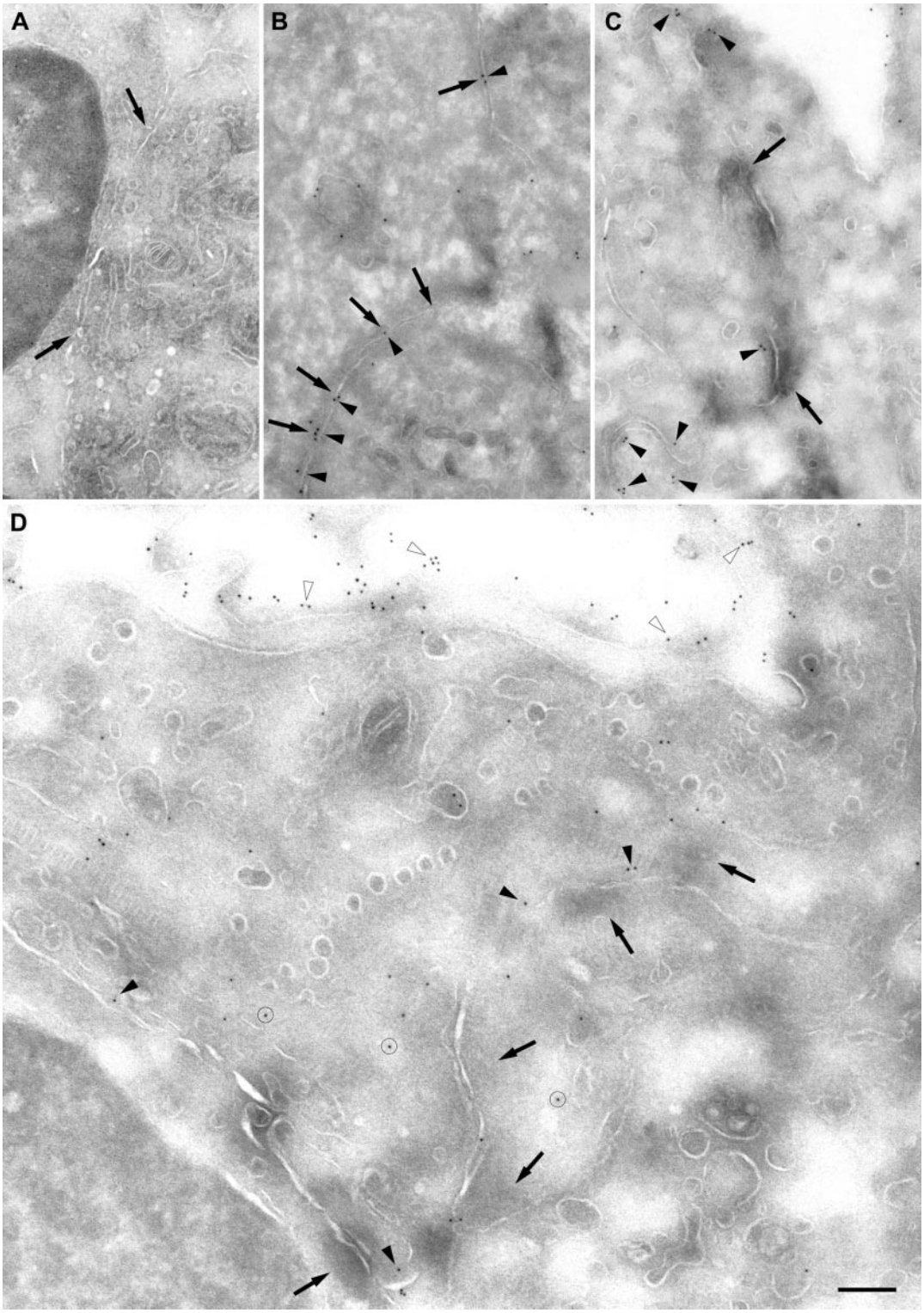

Figure 8. Anti-JAM-C antibody H33 redistributes JAM-C away from junctional regions of endothelial cells in vivo. Ultrathin frozen sections of lymphatic regions in lymph nodes from control and anti-JAM-C antibody-treated mice were immunolabeled for JAM-C. (A) After incubation of a section of a control lymph node with a preimmune rabbit serum and a goat serum against rabbit IgG conjugated with gold particles, no staining was observed along the apposed, lateral membranes (arrows) of endothelial cells. (B–D) Labeling of lymph node sections with immune serum against JAM-C resulted in a specific staining of lateral membranes, shown here in an apical (top) to basal orientation (bottom), in both control and H33-treated lymph nodes. (B) In control lymph node, most junctional regions (arrows) were immunolabeled for JAM-C (arrowheads). (C) In a lymph node from a mouse treated with the H33 antibody, JAM-C (arrowheads) was usually not detected at junctional regions (arrows), but was evident in nearby, nonjunctional regions of the same lateral membrane (arrowheads). (D) JAM-C was immunodetected in the cytoplasm (circled), at the apical membrane of endothelial cells (open arrow heads), and at lateral cell-to-cell interfaces (solid arrow heads). Bars, 200 nm in A–C, 400 nm in D.

Table 1. Morphometric data evaluating JAM-C immunolabeling of endothelial cells of lymph nodes

	No. of gold particles per μm^2 cytoplasm	No. of gold particles per μm membrane	No. of gold particles per junctional membrane	JAM-C-labeled junctional membranes (%)
Control mAb	7.81 ± 0.60[a] (n = 39)	1.67 ± 0.13[a] (n = 156)	1 (0–6)[b] (n = 143)	67.1 (96/143)
H33 mAb	8.64 ± 0.77[a] (n = 45)	2.10 ± 0.13[ac] (n = 259)	0 (0–4)[bd] (n = 164)	17.7 (29/164)

The distribution of JAM-C immunolabeling was assessed on 40 randomly selected endothelial cells, taken in similar numbers in at least 3 different lymph nodes of two animals per group. Measures were performed on 453 μm (control mAb) and 510 μm (H33 antibody) of plasma membrane, as well as on 297 μm^2 (control mAb) and 494 μm^2 (H33 antibody) of cytoplasm. After scoring the number of gold particles over the measured compartments, we calculated the number of particles per μm of membrane and μm^2 of cytoplasm. We further evaluated the distribution of gold particles over the junctional portions of the cell membrane, which were identified by a narrowing of the intercellular space between two adjacent cell membranes associated to an accumulation of microfilaments on the cytoplasmic sides.

[a] Data are shown as mean ± SEM, due to the normal distribution of these parameters. Differences between the control and the H33-treated group were evaluated by either analysis of variance or nonparametric tests, whichever was applicable.

[b] Data are shown as median values (with range in parentheses), due to the asymmetric distribution of these parameters. Differences between the control and the H33-treated group were evaluated by either analysis of variance or nonparametric tests, whichever was applicable.

[c] $p < 0.03$, [d] $p < 0.001$. Values in parentheses are number of cells, membranes, and junctional regions scored.

PATJ, and ZO-1 associate with JAM-C (Ebnet *et al.*, 2003; Gliki *et al.*, 2004), suggesting that junctional polarity complexes stabilize JAM-C in junctions in the absence of JAM-B.

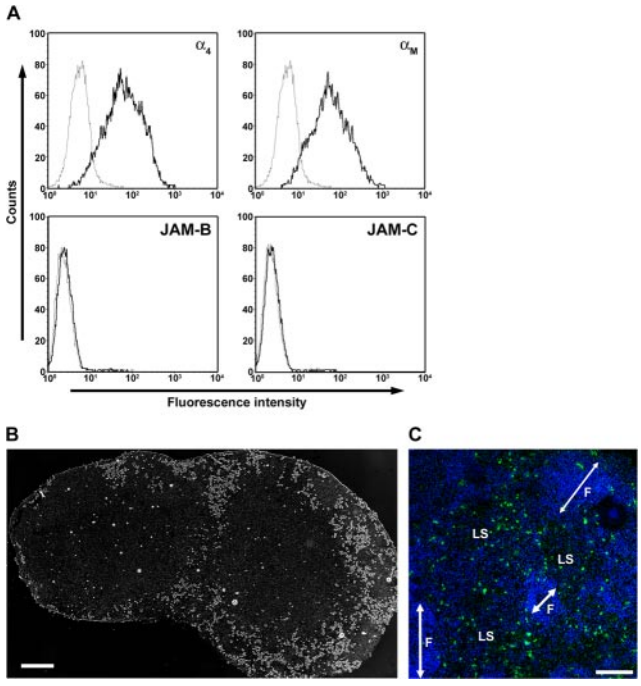

Figure 9. Leukocyte adhesion to frozen section of lymph nodes (Stamper-Woodruff assay). (A) Surface expression of the indicated adhesion molecules by WEHI78/24 monocytoid cell line were detected by flow cytometry using monoclonal antibodies against α_4 integrin (PS/2), α_M integrin (M1/70), or polyclonal sera against murine JAM-B and JAM-C. Plain profiles show the surface expression, whereas dashed profiles show the appropriate isotype matched controls for rat monoclonal antibodies or preimmune rabbit sera. (B) Representative image of lymph node section to which the monocytoid cell line labeled with calcein adhered for 30 min at 37°C. Most of the fluorescent monocytes adhered to subcapsular areas typical of lymphatic sinuses. Scale bar, 250 μm. (C) Higher magnification of lymph node section (nuclei stained in blue) after adhesion of calcein-labeled monocytoid cells (green). F, follicles; LS, lymphatic sinuses. Scale bar, 100 μm.

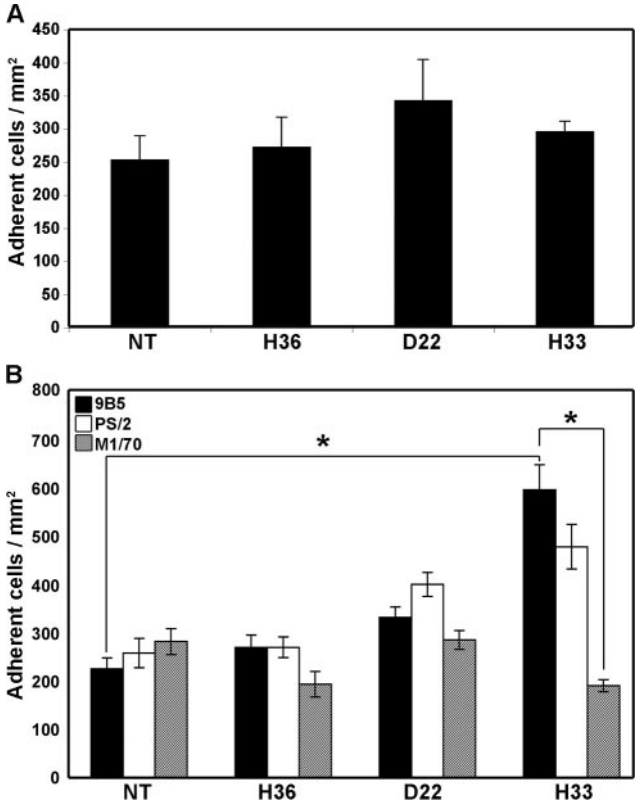

Figure 10. Treatment of mice with antibodies to JAM-C increases monocyte adhesion to lymph node sections in Stamper and Woodruff assays. (A) Stamper and Woodruff assay was performed on lymph node sections obtained from nontreated animals. WEHI78/24 cells were incubated in the presence or absence of indicated anti-JAM-C antibodies. In these conditions anti-JAM-C antibodies do not affect the adhesion of monocytoid cells to lymph node sections. (B) Stamper and Woodruff adhesion assay was done on lymph node sections from mice treated with H36, D22, H33, or isotype-matched control antibodies. As shown, H33 antibody increases the adhesion of monocytoid cells when administrated to mice. Experiments were done in the presence of blocking antibodies against α_4 integrin (PS/2, white columns), against α_M integrin (M1/70, dashed columns) or isotype-matched control antibody (black columns). Data shown are the mean ± SEM of the number of adhering cells/mm^2 found on eight sections per lymph nodes in three animals per condition. * $p < 0.05$.

JAM-B Modulates JAM-C Interaction with the Leukocyte Integrin $\alpha_M\beta_2$

We show that JAM-B, by interacting with JAM-C, modulates the accessibility of JAM-C for $\alpha_M\beta_2$ integrin-mediated adhesion of the monocytoid cell line WEHI78/24 to lymph node sections. According to previous reports, the monocytoid cells do not adhere to noninflamed HEVs in Stamper and Woodruff assays, but prominently bind to lymphatic sinuses (Stamper and Woodruff, 1976; McEvoy *et al.*, 1997). Antibodies against JAM-C do not affect this adhesion. In contrast, the blockade of JAM-B/JAM-C interaction in vivo relocalizes JAM-C and makes it available for the monocyte integrin $\alpha_M\beta_2$. We also observe the relocalization of JAM-C upon H33 antibody treatment on mixed monolayers of JAM-B- and JAM-C-transfected CHO cells (unpublished data). Unfortunately, WEHI78/24 cells poorly adhere to mixed monolayers, impairing a correlative study between JAM-C localization and leukocyte adhesion in vitro. This experimental limitation is consistent with previous findings showing that CHO cells do not support leukocyte adhesion in the absence of VCAM-1 and E-selectin expression (Cinamon *et al.*, 2001).

The interaction of JAM-A with the integrin LFA-1 has also been suggested to require prior relocalization of JAM-A from intercellular junctions to the apical surface (Ostermann *et al.*, 2002; Ebnet *et al.*, 2004). Indeed, treatment of endothelial cells with a combination of TNF-α and INF-γ redistributes JAM-A away from cell-cell contacts. This indicates that under inflammatory conditions, JAM-A becomes available at the apical surface of endothelial cells for LFA-1-mediated leukocyte adhesion (Ozaki *et al.*, 1999; Ebnet *et al.*, 2004). Similarly, our results suggest that $\alpha_M\beta_2$-mediated adhesion of monocytes to JAM-C is regulated by its delocalization to the apical surface of endothelial cells. However, the antibody treatment may also affect homodimerization of JAM-C or *cis*-interaction between JAM-C and another endothelial counterreceptor for $\alpha_M\beta_2$ integrin. Indeed, the study of animals deficient for JAM-A expression has shown that JAM-A increases spreading and migration in a cell autonomous manner (Cera *et al.*, 2004). Indeed, GSK-3β inhibition reverses the motile activity observed in cells deficient for JAM-A, establishing a link between JAM-A and protein kinase Cζ/GSK-3β signaling pathways (Bazzoni *et al.*, 2005). Because some intracellular signaling pathways may be common to all JAM family members (Ebnet *et al.*, 2004), we cannot exclude that JAM-A may interfere with the adhesion process described here.

Because JAM-B and JAM-C are respective ligands for the leukocyte integrins $\alpha_4\beta_1$ and $\alpha_M\beta_2$ in human (Cunningham *et al.*, 2002; Santoso *et al.*, 2002), we wonder whether antibody blocking of JAM-B/JAM-C interaction will allow binding of $\alpha_4\beta_1$ integrin to JAM-B. However, the interaction between $\alpha_4\beta_1$ integrin and JAM-B is restricted to cells that coexpress the $\alpha_4\beta_1$ integrin and JAM-C (Cunningham *et al.*, 2002). JAM-C is not expressed on the monocytoid cell line WEHI78/24 and on circulating myeloid cells in mice (Aurrand-Lions *et al.*, 2005). We can thus exclude that H33 antibody favors JAM-B/$\alpha_4\beta_1$ integrin interaction. In addition, the adhesion of monocytoid cells to lymph nodes via $\alpha_M\beta_2$ is exclusively observed upon treatment of mice with the antibody against JAM-C. Thus, the H33 antibody does not hamper the interaction between $\alpha_M\beta_2$ and JAM-C.

To date, the integrin $\alpha_M\beta_2$ has been mostly implicated in the migration of myeloid cells to inflammatory sites (Carlos and Harlan, 1994). Although the most important counterreceptors for $\alpha_M\beta_2$ integrin are ICAM-1 and ICAM-2, other nonidentified ligands on endothelial cells may exist (Issekutz *et al.*, 1999). We propose that a mechanism dependent on leukocyte $\alpha_M\beta_2$ integrin interaction with endothelial JAM-C mediates monocyte adhesion to lymphatic vessels and that the redistribution of the JAM-C participates to this mechanism.

ACKNOWLEDGMENTS

We thank Dominique Ducrest-Gay, Claude Magnin, Patricia Ropraz, and Philippe Hammel for their technical expertise. We are grateful to Dr. Paul Frederick Bradfield for critical reading of the manuscript and helpful advices. The Real-Time quantitative PCR experiments were performed at the Genomics Platform of the National Center of Competence in Research Frontiers in Genetics, with the help of Dr. Mylène Docquier. The analytical ultracentrifugation experiments were performed in the AUC facility established by the Biotechnology and Biological Sciences Research Council and the Wellcome Trust in the Glycobiology Institute of the University of Oxford and managed by Russell Wallis. This work was supported by grants from the Swiss National Science Foundation (M.A.L., 3100.067896.02 and B.A.I., 3100A0.100697/1) and Oncosuisse (OCS-01335-02-2003). E.Y.J. is a Cancer Research UK Principal Research Fellow. P.M. and P.R. are supported by grants from the Swiss National Science Foundation (31-67788.02), the Juvenile Diabetes Research Foundation International (1-2005-46), the European Union (QLRT-2001-01777), and the National Institutes of Health (1RO1 DK-63443-01).

REFERENCES

Altamirano, M. M., Woolfson, A., Donda, A., Shamshiev, A., Briseno-Roa, L., Foster, N. W., Veprintsev, D. B., De Libero, G., Fersht, A. R., and Milstein, C. (2001). Ligand-independent assembly of recombinant human CD1 by using oxidative refolding chromatography. Proc. Natl. Acad. Sci. USA *98*, 3288–3293.

Arrate, M. P., Rodriguez, J. M., Tran, T. M., Brock, T. A., and Cunningham, S. A. (2001). Cloning of human junctional adhesion molecule 3 (JAM3) and its identification as the JAM2 counter-receptor. J. Biol. Chem. *276*, 45826–45832.

Aurrand-Lions, M., Duncan, L., Ballestrem, C., and Imhof, B. A. (2001a). JAM-2, a novel Ig superfamily molecule, expressed by endothelial and lymphatic cells. J. Biol. Chem. *276*, 2733–2741.

Aurrand-Lions, M., Johnson-Leger, C., Wong, C., Du Pasquier, L., and Imhof, B. A. (2001b). Heterogeneity of endothelial junctions is reflected by differential expression and specific subcellular localization of the three JAM family members. Blood *98*, 3699–3707.

Aurrand-Lions, M., Lamagna, C., Dangerfield, J. P., Wang, S., Herrera, P., Nourshargh, S., and Imhof, B. A. (2005). Junctional adhesion molecule-C regulates the early influx of leukocytes into tissues during inflammation. J. Immunol. *174*, 6406–6415.

Aurrand-Lions, M. A., Duncan, L., Du Pasquier, L., and Imhof, B. A. (2000). Cloning of JAM-2 and JAM-3, an emerging junctional adhesion molecular family? Curr. Top. Microbiol. Immunol. *251*, 91–98.

Axelrod, D., Koppel, D. E., Schlessinger, J., Elson, E., and Webb, W. W. (1976). Mobility measurement by analysis of fluorescence photobleaching recovery kinetics. Biophys. J. *16*, 1055–1069.

Bazzoni, G., Martinez-Estrada, O. M., Mueller, F., Nelboeck, P., Schmid, G., Bartfai, T., Dejana, E., and Brockhaus, M. (2000a). Homophilic interaction of junctional adhesion molecule. J. Biol. Chem. *275*, 30970–30976.

Bazzoni, G., Martinez-Estrada, O. M., Orsenigo, F., Cordenonsi, M., Citi, S., and Dejana, E. (2000b). Interaction of junctional adhesion molecule with the tight junction components ZO-1, cingulin, and occludin. J. Biol. Chem. *275*, 20520–20526.

Bazzoni, G., Tonetti, P., Manzi, L., Cera, M. R., Balconi, G., and Dejana, E. (2005). Expression of junctional adhesion molecule-A prevents spontaneous and random motility. J. Cell Sci. *118*, 623–632.

Berg, E. L., Robinson, M. K., Warnock, R. A., and Butcher, E. C. (1991). The human peripheral lymph node vascular addressin is a ligand for LECAM-1, the peripheral lymph node homing receptor. J. Cell Biol. *114*, 343–349.

Carlos, T. M., and Harlan, J. M. (1994). Leukocyte-endothelial adhesion molecules. Blood *84*, 2068–2101.

Cera, M. R. *et al.* (2004). Increased DC trafficking to lymph nodes and contact hypersensitivity in junctional adhesion molecule-A-deficient mice. J. Clin. Invest. *114*, 729–738.

Chavakis, T., Keiper, T., Matz-Westphal, R., Hersemeyer, K., Sachs, U. J., Nawroth, P. P., Preissner, K. T., and Santoso, S. (2004). The junctional adhe-

sion molecule-C promotes neutrophil transendothelial migration in vitro and in vivo. J. Biol. Chem. *279*, 55602–55608.

Cinamon, G., Shinder, V., and Alon, R. (2001). Shear forces promote lymphocyte migration across vascular endothelium bearing apical chemokines. Nat. Immunol. *2*, 515–522.

Cunningham, S. A., Arrate, M. P., Rodriguez, J. M., Bjercke, R. J., Vanderslice, P., Morris, A. P., and Brock, T. A. (2000). A novel protein with homology to the junctional adhesion molecule. Characterization of leukocyte interactions. J. Biol. Chem. *275*, 34750–34756.

Cunningham, S. A., Rodriguez, J. M., Arrate, M. P., Tran, T. M., and Brock, T. A. (2002). JAM2 interacts with alpha4beta1. Facilitation by JAM3. J. Biol. Chem. *277*, 27589–27592.

Ebnet, K., Aurrand-Lions, M., Kuhn, A., Kiefer, F., Butz, S., Zander, K., Meyer zu Brickwedde, M. K., Suzuki, A., Imhof, B. A., and Vestweber, D. (2003). The junctional adhesion molecule (JAM) family members JAM-2 and JAM-3 associate with the cell polarity protein PAR-3, a possible role for JAMs in endothelial cell polarity. J. Cell Sci. *116*, 3879–3891.

Ebnet, K., Schulz, C. U., Meyer Zu Brickwedde, M. K., Pendl, G. G., and Vestweber, D. (2000). Junctional adhesion molecule interacts with the PDZ domain-containing proteins AF-6 and ZO-1. J. Biol. Chem. *275*, 27979–27988.

Ebnet, K., Suzuki, A., Ohno, S., and Vestweber, D. (2004). Junctional adhesion molecules (JAMs): more molecules with dual functions? J. Cell Sci. *117*, 19–29.

Fraemohs, L., Koenen, R. R., Ostermann, G., Heinemann, B., and Weber, C. (2004). The functional interaction of the beta2 integrin lymphocyte function-associated antigen-1 with junctional adhesion molecule-A is mediated by the I domain. J. Immunol. *173*, 6259–6264.

Gliki, G., Ebnet, K., Aurrand-Lions, M., Imhof, B. A., and Adams, R. H. (2004). Spermatid differentiation requires the assembly of a cell polarity complex downstream of junctional adhesion molecule-C. Nature *431*, 320–324.

Ikemizu, S., Gilbert, R. J., Fennelly, J. A., Collins, A. V., Harlos, K., Jones, E. Y., Stuart, D. I., and Davis, S. J. (2000). Structure and dimerization of a soluble form of B7–1. Immunity *12*, 51–60.

Issekutz, A. C., Rowter, D., and Springer, T. A. (1999). Role of ICAM-1 and ICAM-2 and alternate CD11/CD18 ligands in neutrophil transendothelial migration. J. Leukoc. Biol. *65*, 117–126.

Kostrewa, D. *et al.* (2001). X-ray structure of junctional adhesion molecule: structural basis for homophilic adhesion via a novel dimerization motif. EMBO J. *20*, 4391–4398.

Lamagna, C., Hodivala-Dilke, K. M., Imhof, B. A., and Aurrand-Lions, M. (2005). Antibody against junctional adhesion molecule C inhibits angiogenesis and tumor growth. Cancer Res. *65*, 5703–5710.

Laschinger, M., and Engelhardt, B. (2000). Interaction of alpha4-integrin with VCAM-1 is involved in adhesion of encephalitogenic T cell blasts to brain endothelium but not in their transendothelial migration in vitro. J. Neuroimmunol. *102*, 32–43.

Legler, D. F., Wiedle, G., Ross, F. P., and Imhof, B. A. (2001). Superactivation of integrin alphavbeta3 by low antagonist concentrations. J. Cell Sci. *114*, 1545–1553.

Liang, T. W. *et al.* (2002). Vascular endothelial-junctional adhesion molecule (VE-JAM)/JAM 2 interacts with T, NK, and dendritic cells through JAM 3. J. Immunol. *168*, 1618–1626.

Liou, W., Geuze, H. J., and Slot, J. W. (1996). Improving structural integrity of cryosections for immunogold labeling. Histochem. Cell Biol. *106*, 41–58.

Malergue, F., Galland, F., Martin, F., Mansuelle, P., Aurrand-Lions, M., and Naquet, P. (1998). A novel Ig superfamily junctional molecule expressed by antigen presenting cells, endothelial cells and platelets. Mol. Immunol. *35*, 1111–1119.

Martin-Padura, I. *et al.* (1998). Junctional adhesion molecule, a novel member of the Ig superfamily that distributes at intercellular junctions and modulates monocyte transmigration. J. Cell Biol. *142*, 117–127.

McEvoy, L. M., Jutila, M. A., Tsao, P. S., Cooke, J. P., and Butcher, E. C. (1997). Anti-CD43 inhibits monocyte-endothelial adhesion in inflammation and atherogenesis. Blood *90*, 3587–3594.

Ostermann, G., Weber, K. S., Zernecke, A., Schroder, A., and Weber, C. (2002). JAM-1 is a ligand of the beta(2) integrin LFA-1 involved in transendothelial migration of leukocytes. Nat. Immunol. *3*, 151–158.

Ozaki, H., Ishii, K., Horiuchi, H., Arai, H., Kawamoto, T., Okawa, K., Iwamatsu, A., and Kita, T. (1999). Cutting edge: combined treatment of TNF-alpha and IFN-gamma causes redistribution of junctional adhesion molecule in human endothelial cells. J. Immunol. *163*, 553–557.

Palmeri, D., van Zante, A., Huang, C. C., Hemmerich, S., and Rosen, S. D. (2000). Vascular endothelial junction-associated molecule, a novel member of the Ig superfamily, is localized to intercellular boundaries of endothelial cells. J. Biol. Chem. *275*, 19139–19145.

Piali, L., Albelda, S. M., Baldwin, H. S., Hammel, P., Gisler, R. H., and Imhof, B. A. (1993). Murine platelet endothelial cell adhesion molecule (PECAM-1)/CD31 modulates beta 2 integrins on lymphokine-activated killer cells. Eur. J. Immunol. *23*, 2464–2471.

Prota, A. E., Campbell, J. A., Schelling, P., Forrest, J. C., Watson, M. J., Peters, T. R., Aurrand-Lions, M., Imhof, B. A., Dermody, T. S., and Stehle, T. (2003). Crystal structure of human junctional adhesion molecule 1, implications for reovirus binding. Proc. Natl. Acad. Sci. USA *100*, 5366–5371.

Roh, M. H., Makarova, O., Liu, C. J., Shin, K., Lee, S., Laurinec, S., Goyal, M., Wiggins, R., and Margolis, B. (2002). The Maguk protein, Pals1, functions as an adapter, linking mammalian homologues of Crumbs and Discs Lost. J. Cell Biol. *157*, 161–172.

Santoso, S., Sachs, U. J., Kroll, H., Linder, M., Ruf, A., Preissner, K. T., and Chavakis, T. (2002). The junctional adhesion molecule 3 (JAM-3) on human platelets is a counterreceptor for the leukocyte integrin Mac-1. J. Exp. Med. *196*, 679–691.

Springer, T., Galfre, G., Secher, D. S., and Milstein, C. (1979). Mac-1, a macrophage differentiation antigen identified by mAb. Eur. J. Immunol. *9*, 301–306.

Stamper, H. B., Jr., and Woodruff, J. J. (1976). Lymphocyte homing into lymph nodes: in vitro demonstration of the selective affinity of recirculating lymphocytes for high-endothelial venules. J. Exp. Med. *144*, 828–833.

Tokuyasu, K. T. (1997). Immuno-cytochemistry on ultrathin cryosections. In: Cells, a Laboratory Manual, vol. 3 (131), ed. D. L. Spector, R. D. Goodman, and L. A. Leinwand, Cold Spring Harbor, NY: Cold Spring Harbor Laboratory Press, 1–27.

Vandesompele, J., De Preter, K., Pattyn, F., Poppe, B., Van Roy, N., De Paepe, A., and Speleman, F. (2002). Accurate normalization of real-time quantitative RT-PCR data by geometric averaging of multiple internal control genes. Genome Biol. *3*, RESEARCH0034.

Wiedle, G., Johnson-Leger, C., and Imhof, B. A. (1999). A chimeric cell adhesion molecule mediates homing of lymphocytes to vascularized tumors. Cancer Res. *59*, 5255–5263.

Wong, C. W., Wiedle, G., Ballestrem, C., Wehrle-Haller, B., Etteldorf, S., Bruckner, M., Engelhardt, B., Gisler, R. H., and Imhof, B. A. (2000). PECAM-1/C.D31 trans-homophilic binding at the intercellular junctions is independent of its cytoplasmic domain; evidence for heterophilic interaction with integrin alphavbeta3 in Cis. Mol. Biol. Cell *11*, 3109–3121.

Yguerabide, J., Schmidt, J. A., and Yguerabide, E. E. (1982). Lateral mobility in membranes as detected by fluorescence recovery after photobleaching. Biophys. J. *40*, 69–75.